

# Velocity field in cluster outskirts in $\Lambda$ CDM models

Maximiliano C. Pivato<sup>1</sup>, N. D. Padilla<sup>2</sup> and D. G. Lambas<sup>1</sup>

<sup>1</sup>Grupo IATE, Observatorio Astronómico de Córdoba, UNC, Argentina email:  
maxip@oac.uncor.edu; dgl@oac.uncor.edu

<sup>2</sup>Dept. Physics, University of Durham, South Road, Durham, DH1 3LE, UK email:  
n.d.padilla@durham.ac.uk

**Abstract.** We analyse statistically the infall of mass onto clusters in  $\Lambda$ -CDM numerical simulations. Also, we consider numerical simulations which include galaxy formation through semi-analytical models to compare the expected infall of mass and galaxies. We find the most probable values at  $V \sim 300\text{--}400$  km/s and a significant tail of large infall velocities ( $V > 1000$  km/s). The flow onto cluster is more pronounced for high local density regions. Mass and galaxies behave similarly although with a slightly lower amplitude.

---

## 1. Introduction

The dynamical behaviour of objects near regions of high density contrast can be described by the spherical infall model with a collapsing streaming motion with amplitude depending only on the distance to the local density maximum (Diaferio & Geller 1997). Assuming linear theory,  $v_p(r) = -1/3\Omega_0 H_0 r \delta(r)$ ; in the non-linear regime, Rêgos & Geller (1989) find an approximate solution given by  $v_p(r) = -1/3\Omega_0 H_0 r \delta(r)/[\delta(r)+1]^{0.25}$  which slightly improve the agreement with simulations (Croft, Dalton & Efstathiou 1999). Here, we explore the characteristics of streaming motions in cluster vicinity using large high-resolution N-body simulations (VLS) carried out by the Virgo Supercomputing Consortium. VLS simulations consider a  $\Lambda$ -CDM primordial spectrum ( $\Omega_\Lambda = 0.7$ ,  $\Omega_m = 0.3$ ,  $h = 0.7$ ) in a  $479h^{-1}$ Mpc box size with resolution  $6.8 \times 10^{10} M_\odot$ .

## 2. Analysis

In figure 1, we show the results of the mass infall onto the most massive clusters in the simulation box. The arrows indicate the velocity flow where it can be clearly appreciated the systematic infall around the most prominent clusters.

The histograms of figure 2 show the distribution of the cluster-centric component of the peculiar velocities of particles at different distances from the most massive clusters ( $M > 10^{14} M_\odot$ ) in the simulation. It can be seen the large spread of velocities and the shift of the mean values toward negative velocities by an amount of  $v \sim 200$  km/s.

The distributions corresponding to the net infall at a given cluster-centric distance are displayed in figure 3. It can be appreciated the non gaussianity of the distribution of infall velocities regardless of the distance to the cluster. The distributions show the most probable values  $V \sim 200\text{--}400$  km/s and the tails of large infalling velocities,  $V > 1000$  km/s.

We expect the amplitude of the infall velocities at a given distance from the group center to increase monotonically with cluster mass. Therefore, we have explored the mean infall at different distances to clusters with a range of masses  $M < 1.1 \times 10^{13} M_\odot$

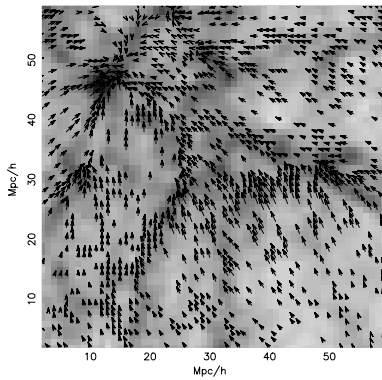


**Figure 1.** Infall pattern in a typical region of the simulation box.

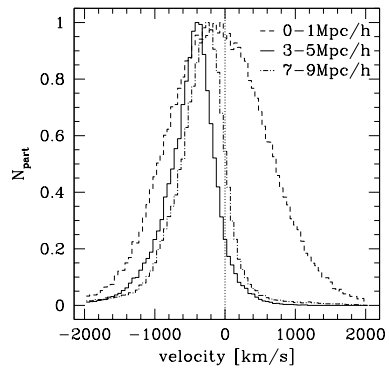


**Figure 2.** Distribution of particle velocities in the direction to cluster centers, normalized to the maximum values.

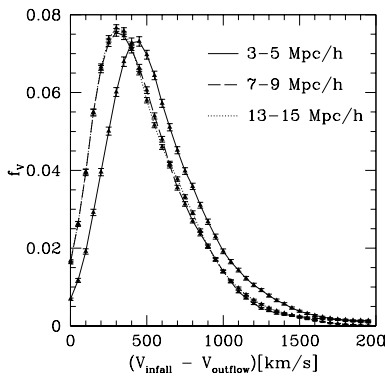


**Figure 3.** Distribution of the net infall velocities.

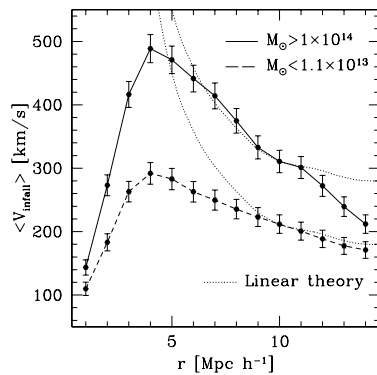


**Figure 4.** Mean infall velocities as a function of distance for two ranges of cluster masses.

and  $M > 10^{14}M_{\odot}$ . The results displayed in figure 4 show a significant increase of the maximum infall amplitude onto the most massive clusters on scales  $r \sim 4h^{-1}\text{Mpc}$ .

We also explored the variation of the infall pattern according to the local particle density, smoothed on  $3h^{-1}\text{Mpc}$  scale, appropriate to consider the collapsing streaming motions onto clusters from different regions such as filaments or voids. In figure 5 are shown the results, where it can be appreciated that particles in high density regions flow most rapidly onto large mass concentrations than those in underdense environments.

Finally, we have considered a high resolution N-body simulation populated with galaxies using the semi-analytic model, GALFORM (Cole et al. 2000; Benson et al. 2002). The simulation uses standard  $\Lambda$ CDM parameters, with normalization given by  $\sigma_8 = 0.80$  and a primordial spectral index of  $n = 0.97$ . The N-body simulation box is  $250h^{-1}\text{Mpc}$  on a side and contains  $1.25 \times 10^8$  dark matter particles of mass  $1.04 \times 10^{10}h^{-1}M_{\odot}$ .

Figure 6 shows the mean infall velocity of DM particles and semi-analytic galaxies in the simulation cube, as a function of distance to cluster centres. We show results for the full sample of semi-analytic galaxies and for those with absolute magnitudes  $B_j < -18$ . This figure shows the results for subsamples of haloes defined using different lower mass limits. As can be seen, galaxies show a behaviour similar to DM particles even when restricting to brighter galaxies, although infall velocities seem to be marginally lower for galaxies than for the dark matter.

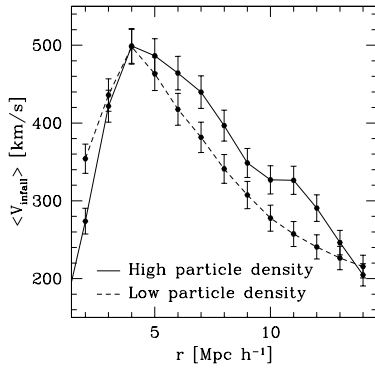


**Figure 5.** Distribution of net infall velocities for particles in high (solid line) and low (dashed line) density regions.

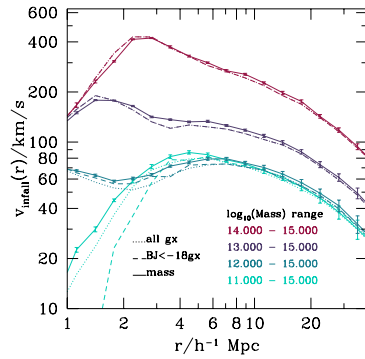


**Figure 6.** Mean infall for galaxies and dark matter particles in semianalytical models.

### Acknowledgements

MP and DL acknowledge kind support from Dr. Antonaldo Diaferio to attend the IAU Colloquium 195.

### References

- Benson A.J., Lacey C.G., Baugh C.M., Cole S. & Frenk C.S. 2002 *Mon. Not. R. Astr. Soc.* **333**, 156–176.
- Cole S., Lacey C.G., Baugh C.M., & Frenk C.S. 2000 *Mon. Not. R. Astr. Soc.* **319**, 168–204.
- Croft R.A.C., Dalton G.B. & Efstathiou G. 1999 *Mon. Not. R. Astr. Soc.* **305**, 547–562.
- Diaferio A. & Geller M.J. 1997 *Astrophys. J.*, **481**, 633–643.
- Régos E. & Geller M.J. 1989 *Astr. J.*, **98**, 755–765.